33rd Annual International Conference of the IEEE EMBS
Boston, Massachusetts USA, August 30 - September 3, 2011

Principle Component Analysis on Photoplethysmograms: Blood Oxygen Saturation Estimation and Signal Segmentation

Kejia Li, *Student Member, IEEE* and Steve Warren, *Member, IEEE*

***Abstract*—Most pulse oximeters determine blood oxygen saturation (SpO_2) after calculating a coefficient, *R*, that represents the normalized ratiometric contributions of the pulsatile red and near-infrared photoplethysmograms (PPGs) acquired by the sensor. This paper presents a new approach that uses principle component analysis (PCA) to separate the signal and noise components of unfiltered PPGs and provide the determination of *R*. Also, rather than use peak-to-valley time intervals to obtain *R*, this technique uses eigenvalue and eigenvector data obtained during PCA to optimize these time intervals and improve the *R* calculation. Early analyses on unfiltered PPGs from 16 subjects indicate that these *R* values compare to those obtained from FFT-based methods and yield SpO_2 values consistent with those reported by a commercial unit. All signal data are considered during the PCA process, so this technique shows promise to precisely segment clean versus noise-corrupted PPGs.**

***Keywords*—artifact, optimization, photoplethysmogram, principle component analysis, pulse oximetry, segmentation**

I. Introduction

OXIMETER history can be traced back to 1942, when Glenn Allen Millikan developed the first noninvasive optical device to estimate oxygen saturation in hemoglobin [1]. In 1972, Takuo Aoyagi developed what was known as the pulse oximeter, which obtained a quantity directly related to oxygen saturation in arterial blood (SpO_2) by analyzing the pulsatile component of light absorption in perfused tissue at red versus infrared wavelengths [2]. Beer-Lambert's law [2] relates to this analysis, requiring that *n* equations (data from *n* wavelengths of light) be solved to obtain *n* solute concentrations (hemoglobin derivatives).

In most pulse oximeters, two excitation wavelengths help to determine a normalized ratio of pulsatile absorption values – a ratio that plays a role in a linear calibration curve for oxygen saturation values between 70% and 100% [3]. For a CO-oximeter, additional wavelengths allow one to calculate, e.g., carboxyhemoglobin concentration [4]. A normalized ratiometric coefficient, *R*, is the key component in SpO_2 calculation. Methods to calculate *R* include 1) signal amplitude extraction from pulsatile waveforms, 2) Fourier transformation of pulsatile waveforms to extract the peak of each fundamental harmonic [5], and 3) independent component analysis (ICA) [6], e.g., the Discrete Saturation Transform used by Masimo Corporation [7].

This paper presents a new method to estimate SpO_2 from unfiltered PPGs, where two optimization strategies are employed. It also demonstrates that the PCA method offers a potential means to segment corrupted versus clean PPG data.

II. Methods

A. Experimental Measurements and Parameter Definitions

A custom wireless reflectance pulse oximeter [8] was used to acquire fingertip PPG data from 16 subjects. The two-channel pulse oximeter (red at 660 nm, near-infrared at 910 nm) yields four unfiltered PPG data streams (AC_{red}, DC_{red}, AC_{ir}, DC_{ir}) at a sampling frequency of f_s = 240 Hz (see Fig. 1). Each signal (pulsatile AC signal or DC baseline) offers up to 4096 digitization levels (range: 0–2.4 V). Note that the DC baseline is assumed to be constant in some pulse oximeters [9] or adjustable based on tissue perfusion level (i.e., the design employed here). While the DC signals used here are not constant, they usually occupy a limited range. This custom unit uses a compensation method afterwards to address discontinuities in the AC signal caused by immediate adjustments in the DC level [8].

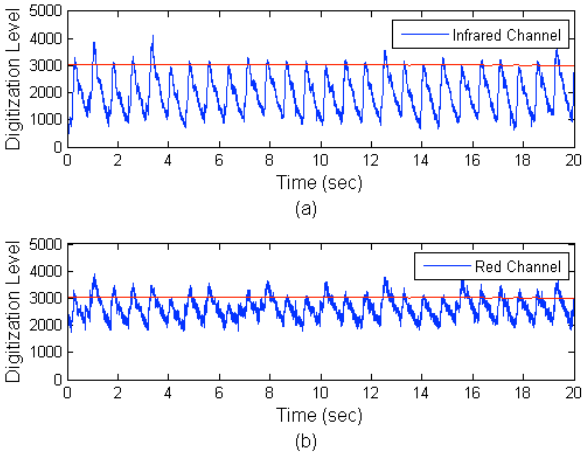

Fig. 1. Twenty seconds of representative raw fingertip PPGs: (a) near-infrared and (b) red. Each channel contains AC and DC data.

SpO_2 calculation usually involves the coefficient $R = (I_{AC}/I_{DC})_{red}/(I_{AC}/I_{DC})_{ir}$, where I_{AC} is the peak-to-valley excursion of the pulsatile portion of a PPG and I_{DC} is the corresponding baseline. An experimentally determined linear calibration curve, SpO_2 (%) = $a \times R + b$, is then

Manuscript received March 26, 2011; accepted June 8, 2011. This work was supported in part by the National Science Foundation under grants BES–0093916, CNS–0932289, and CNS–0551626. Findings, conclusions, or recommendations expressed in this material are those of the author(s) and do not necessarily reflect the views of the NSF.

Kejia Li and Steve Warren are with the Department of Electrical & Computer Engineering, Kansas State University, Manhattan, KS 66506, USA (kejiali@ksu.edu; swarren@ksu.edu).

employed, where (a, b) is a constant-coefficient pair such as (–25, 110) [10]. In this paper, we redefined R as

$$R(i) = \frac{\{x_{AC}(i) / I_{DC}\}_{red}}{\{x_{AC}(i) / I_{DC}\}_{ir}} \quad (1)$$

where $x_{AC}(i)$ is a red or near-infrared AC excursion at the i^{th} point that is not restricted to a peak/valley point.

B. Principle Component Analysis (PCA)

PCA orthogonally transforms a number of correlated variables (observations) into a number of uncorrelated variables (sources). Two observations, $\{x_{AC}(i)\}_{red}$ and $\{x_{AC}(i)\}_{ir}$, as defined in (1), are SpO_2-correlated since the I_{DC} ratio is either preset or automatically adjusted based on the subject's perfusion level.

First, we define the $M \times N$ ($M = 2$) data matrix

$$X = \begin{bmatrix} \underline{x}_1 & \underline{x}_2 & \dots & \underline{x}_N \end{bmatrix} \quad (2)$$

where $\underline{x}_i = [\{x_{AC}(i)\}_{ir} \{x_{AC}(i)\}_{red}]^T$, $i = 1, 2, \dots, N$ and N is the number of data points acquired from each channel. The differential value $x_{AC}(i)$ is defined as

$$x_{AC}(i) = \mathrm{AC}(i) - \mathrm{AC}(i+d) \quad (3)$$

where AC(i) is the i^{th} point in the red or near-infrared channel and d is the time slot width.

PCA identifies the source matrix, S, with the expression

$$S^T = X^T W \quad (4)$$

where $S = [S_{ppg} S_{noise}]^T$ holds an N-point PPG signal sequence (S_{ppg}) and an N-point noise sequence (S_{noise}), X is the data matrix in (2), and W is an $M \times M$ transformation matrix.

The covariance method can determine W. First, calculate the zero empirical mean data set, B ($M \times N$):

$$B = X - \frac{1}{N} \sum_{i=1}^{N} \underline{x}_i \cdot h \quad (5)$$

where h is a $1 \times N$ vector: $h[n] = 1$ for $n = 1, 2, \dots, N$.

Next, find the empirical covariance matrix ($M \times M$)

$$C = \frac{1}{N} \sum B \cdot B^T \quad (6)$$

and the eigenvectors and eigenvalues of C according to

$$V^{-1} C V = D \quad (7)$$

where V is the $M \times M$ eigenvector matrix corresponding to the eigenvalues in the diagonal matrix D. Rearrange V and D according to decreasing eigenvalue order in D to get $W = V$. The first eigenvector in V indicates the direction of the first principle component, S_{ppg}, and the orthogonal second eigenvector in V corresponds to the second principle component, S_{noise}. The overall best-fit x_{AC} ratio is the first eigenvector's slope:

$$\frac{(x_{AC})_{red}}{(x_{AC})_{ir}} = \frac{V(2,1)}{V(1,1)} \quad (8)$$

C. Optimization

A different time delay, d, yields a different x_{AC} ratio since the data in (2) change. When noise exists, not all d values yield a reliable x_{AC} ratio. For example, $d = 1$ equates to taking the derivative of the original PPG – a process that is sensitive to noise. The following two strategies are introduced to find the most reliable x_{AC} ratio, where d is subject to an empirical upper bound of 100 ($100/f_s = 0.417$ sec time slot).

Signal-to-Noise Energy Ratio Maximization (SNERM). The magnitude of each eigenvalue in matrix D represents the contribution of the source data's energy along each eigenvector. Assuming the energy of the clean PPG signal is greater than the energy of the noise in the given data set, d is selected to maximize the SNER:

$$d = \arg\max \frac{D(1,1)}{D(2,2)} \quad (9)$$

Fig. 2 illustrates the SNERM optimization strategy used in this PCA analysis for the data set in Fig. 1. The simulation results are $d = 80$, SNER = 39.4, first eigenvector $v_1 = [0.8883\ 0.4593]^T$, and x_{AC} ratio = 0.5170.

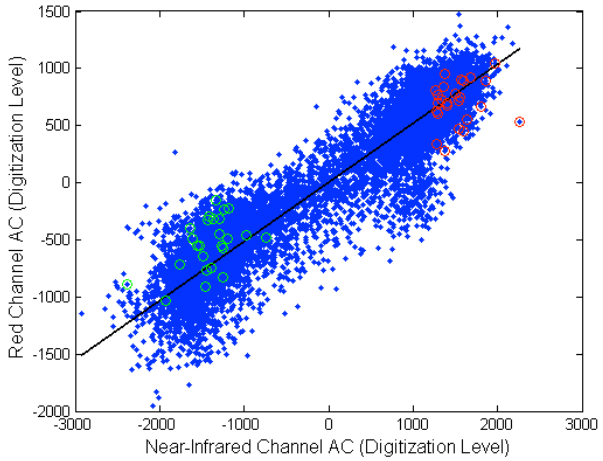

Fig. 2. PCA of a 20-second PPG data set using the optimization strategy of signal-to-noise energy ratio maximization (SNERM). Red circles mark the original peaks, and green circles mark the original valleys.

AC Excursion Ratio Minimization (ACERM). This strategy is based on the idea that the source component S_{ppg} helps to discriminate $(x_{AC})_{ir}$ from $(x_{AC})_{red}$ because the sensor has different responsivity at these two wavelengths. This is coupled with the assumption that the source component S_{noise} imposes the same effect on $(x_{AC})_{ir}$ and $(x_{AC})_{red}$ since, e.g., the same ambient noise is acquired by the sensor during the respective sampling events. The x_{AC} ratio is typically less than 1, so d can be chosen to minimize the ratio in (8):

$$d = \arg\min \frac{V(2,1)}{V(1,1)} \quad (10)$$

Fig. 3 illustrates the ACERM optimization strategy used in this PCA analysis for the same data set in Fig. 1. The simulation results are $d = 68$, SNER = 38.8, first eigenvector $v_1 = [0.8888\ 0.4585]^T$, and ACER or x_{AC} ratio = 0.5155.

Note that no data matrix centering as in (5) is involved in the ACERM strategy so as to prevent an unreasonably low x_{AC} ratio. If mean subtraction is not performed, the first principle component might instead correspond to the mean of the data [11]. However, the method to create the data matrix in (2) and (3) statistically tends toward a near-zero mean, as shown in Fig. 3, and the influence of a small AC mean on the calibration coefficient used for SpO_2 estimation is unclear.

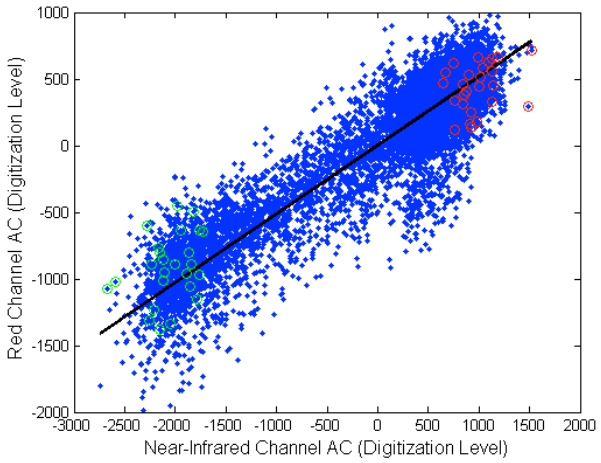

Fig. 3. PCA of a 20-second PPG data set using the optimization strategy of AC excursion ratio minimization (ACERM). Red circles mark the original peaks, and green circles mark the original valleys.

D. Calibration and Agreement Analysis

A commercial pulse oximeter was used as a standard to calibrate the blood oxygen saturation levels obtained from the coefficients determined using the approaches described above. A linear calibration curve as mentioned in *Section A* was then estimated using least-squares approximation [12].

A Bland-Altman plot is a method where data differences are plotted against data averages to assess the agreement between two methods of clinical measurement [13]. For this analysis, comparisons of the calibration coefficient, R, were accomplished by first estimating R for a given data set using the Fast Fourier Transform (FFT) approach (previously noted as reliable [5], [8]) and then calculating R for that same data set using each of the PCA approaches. In the FFT method, R was updated every 0.5 seconds using the previous 4 seconds of data, and a median filter was applied to the resulting coefficient sequence. SNERM and ACERM optimizations were then implemented to create the respective Bland-Altman plots, where the R values determined using these PCA methods were compared against the corresponding FFT-determined coefficients. Separate data sets from 16 participants, each consisting of 40 seconds of four raw PPG data streams, were used to evaluate the effectiveness of the PCA method for estimating SpO_2.

III. Results and Discussion

A. Blood Oxygen Saturation Estimation

SpO_2 levels read from a Smiths Medical BCI® 3180 pulse oximeter are plotted in Fig. 4 as a function of the calibration coefficients calculated with the custom pulse oximeter data using the PCA SNERM and ACERM approaches. The linear calibration curve for the PCA SNERM strategy is

$$SpO_2(\%) = -18.9R + 106.8 \tag{11}$$

with a correlation coefficient, r^2 = 0.77, and a standard deviation, σ = 0.51 (%). The PCA ACERM curve is

$$SpO_2(\%) = -20.2R + 107.4 \tag{12}$$

with a correlation coefficient, r^2 = 0.78, and a standard deviation, σ = 0.50 (%).

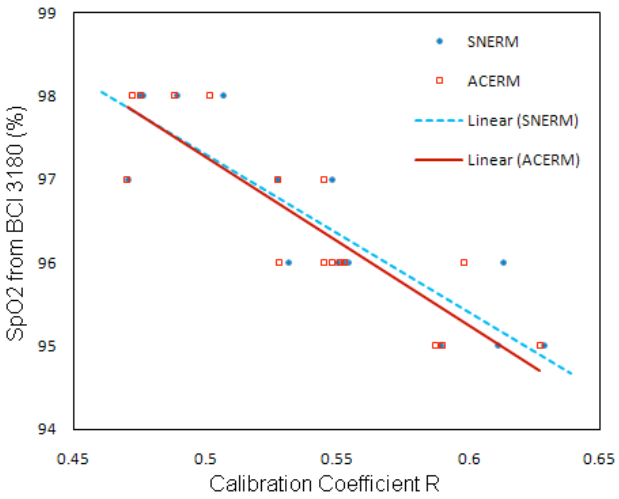

Fig. 4. SpO_2 obtained from a BCI® 3180 pulse oximeter as a function of the R values estimated by the PCA SNERM and ACERM approaches. The SNERM linear regression line (blue dashed line) is SpO_2 (%) = –18.9R + 106.8, and the ACERM line (red solid line) is SpO_2 (%) = –20.2R + 107.4.

B. Blood Oxygen Saturation Agreement

The limits of agreement during Bland-Altman analysis are specified as a mean difference (bias) ±1.96 standard deviations of the difference. As noted in Fig. 5, the agreement between 16 pairs of R estimates as calculated by the FFT method versus the PCA SNERM approach (blue circle, dashed line) is specified by a bias of –0.0109 with agreement limits of –0.0564 to 0.0345. The agreement of the

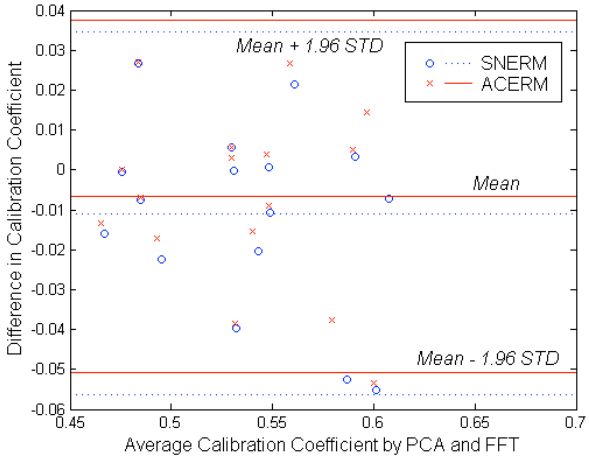

Fig. 5. Bland-Altman plots that note the agreement between 16 pairs of R values calculated with the FFT, PCA SNERM, and PCA ACERM methods.

FFT method versus the PCA ACERM approach (red '×', solid line) is specified by a bias of 0.0066 with agreement limits of –0.0508 to 0.0376.

A strong agreement between the FFT approach and the two PCA approaches was achieved. For instance, using (11) as the calibration curve, the difference in SpO_2 percentage is ensured to be less than 1.07% (18.9×0.0564) between the FFT and SNERM methods. ACERM yields a 40% smaller bias and a 3% narrower limit range as compared to SNERM, consistent with the calibration results (higher r^2 and lower σ).

C. Signal Segmentation for Improved SpO_2 Estimation

Fig. 6 depicts a 20-second data set with partial corruption (segment A). An initial assessment of PCA resistance to the presence of noise was disappointing. This is intuitively reasonable because the limited PPG data present, e.g., in segment A make it impossible to 'create' an SpO_2 indicator by linearly combining the data sequences AC_{red} and AC_{ir}.

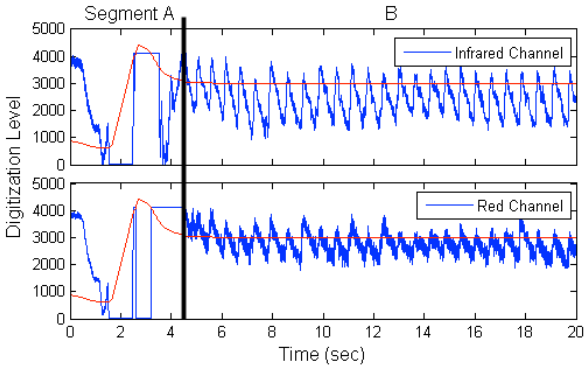

Fig. 6. Twenty seconds of four-channel PPG data segmented into partially corrupted (A) and usable (B) data (transition time: 4.5 sec).

However, it is possible to separate, e.g., the corrupted segment A from the remaining valid data once PCA is performed, as illustrated in Fig. 7. Further separation can be done in segment A according to the signal saturation state: the data were not preprocessed with (3) to make the saturated signal more distinguishable. By culling segment A from the 20-second data set, the initial eigenvector v_1 = $[0.6932\ 0.7207]^T$ becomes $[0.8767\ 0.4810]^T$, yielding a more reasonable SpO_2 estimate. Automatic segmentation based on PCA plots/results and the associated marking of the original time-domain waveforms will be future work.

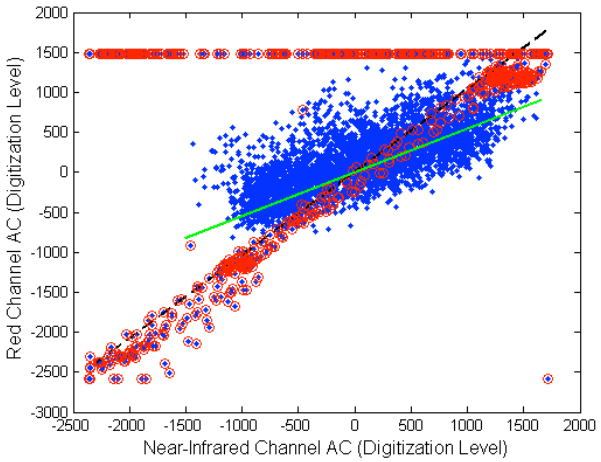

Fig. 7. PCA on the PPG data from Fig. 6: noise-corrupted segment A (⊙) and clean segment B (•).

IV. Conclusion

This paper presented an approach to optimize the calculation of pulse oximeter SpO_2 values by performing PCA on the unfiltered pulsatile PPG data, where the PCA method separates the signal source from the noise source. Two effective strategies are presented to improve the calculation of the conversion coefficient, R, by optimizing the time interval over which these calculations are made, taking advantage of the eigenvalues/eigenvectors ascertained during PCA. These R values are sensible when compared to R values from FFT-based approaches. The PCA results demonstrate resilience to noise and promise to segment noise-corrupted PPG data from clean PPG data. The PCA method can also be applied to an $M > 2$ condition, e.g., for a CO-oximeter.

References

[1] G. A. Millikan, "The Oximeter, an Instrument for Measuring Continuously the Oxygen Saturation of Arterial Blood in Man," *Review of Scientific Instruments,* vol. 13, pp. 434-444, 1942.

[2] K. K. Tremper, "Pulse Oximetry," *Chest,* vol. 95, pp. 713-715, April 1989.

[3] J. G. Webster, *Design of Pulse Oximeters*, 1st ed. New York: Taylor & Francis, 1997.

[4] F. L. Rodkey, T. A. Hill, L. Pitts, and R. F. Robertson, "Spectrophotometric Measurement of Carboxyhemoglobin and Methemoglobin in Blood," *Clinical Chemistry,* vol. 25, pp. 1388-1393, 1979.

[5] J. T. Love, S. Warren, G. R. Laguna, and T. J. Miller, "Personal Status Monitor," Sandia National Laboratories SAND97-0418, UC-706, unlimited release, Feb. 1997.

[6] T. Jensen, S. Duun, J. Larsen, R. G. Haahr, M. H. Toft, B. Belhage, and E. V. Thomsen, "Independent Component Analysis Applied to Pulse Oximetry in the Estimation of the Arterial Oxygen Saturation (SpO2) - a Comparative Study," *31st Annual International Conference of the IEEE EMBS*, Minneapolis, Minnesota, Sept. 2-6, 2009, pp. 4039-4044.

[7] J. M. Goldman, M. T. Petterson, R. J. Kopotic, and S. J. Barker, "Masimo Signal Extraction Pulse Oximetry," *Journal of Clinical Monitoring and Computing,* vol. 16, pp. 475-483, 2000.

[8] K. Li and S. Warren, "A Wireless Reflectance Pulse Oximeter Suitable for Wearable and Surface-Integratable Designs That Produces Unfiltered Photoplethysmograms," *IEEE Transactions on Biomedical Circuits and Systems,* submitted for publication.

[9] S. Rhee, B. H. Yang, and H. Asada, "Artifact-Resistant, Power-Efficient Design of Finger-Ring Plethysmographic Sensors," *IEEE Transactions on Biomedical Engineering,* vol. 48, pp. 795-805, July 2001.

[10] J. E. Scharf, S. Athan, and D. Cain, "Pulse Oximetry Through Spectral Analysis," *12th Southern Biomedical Engineering Conference*, New Orleans, LA, 1993, pp. 227-229.

[11] I. T. Jolliffe, *Principal Component Analysis*, 2nd ed. New York: Springer-Verlag, 2010.

[12] J. G. Proakis, C. M. Rader, F. Ling, C. L. Nikias, M. Moonen, and I. K. Proudler, *Algorithms for Statistical Signal Processing*, 1st ed. New Jersey: Prentice Hall, 2002.

[13] J. M. Bland and D. G. Altman, "Statistical Methods for Assessing Agreement between Two Methods of Clinical Measurement," *Lancet,* pp. 307-310, 1986.